RAPID COMMUNICATIONS

PHYSICAL REVIEW B VOLUME 45, NUMBER 7 15 FEBRUARY 1992-I

Temperature dependence of electronic transitions in MgO, α-Al_2O_3, and α-SiO_2: Final-state effects on phonon coupling

W. L. O'Brien, J. Jia, Q-Y. Dong, and T. A. Callcott
University of Tennessee, Knoxville, Tennessee 37996

D. R. Mueller and D. L. Ederer
National Institute of Standards and Technology, Gaithersburg, Maryland 20899
(Received 28 October 1991; revised manuscript received 5 December 1991)

We present temperature-dependent soft-x-ray emission and soft-x-ray absorption measurements on MgO, α-Al_2O_3, and α-SiO_2. The measurements show in detail the final-state effect on phonon broadening for transitions involving the Mg $2P$ core state in MgO. In addition, we report the temperature dependence of emission and absorption features for MgO, α-Al_2O_3, and α-SiO_2. The temperature dependence of the transitions involving the valence- and conduction-band states should be an important check on band-structure calculations. These results are compared to published temperature-dependent optical-reflectivity measurements.

Phonon effects on electronic transitions have been of interest for over thirty years.[1-6] Ionic solids have played a significant role in this interest due to the simplifying assumptions which can be used.[3,4,7] In ionic solids, phonon broadening much larger than kT have been observed[3] and described theoretically.[4] This broadening is due to strong phonon coupling to the electronic excitations. Temperature-dependent changes in band gaps and other electronic transition energies have also been observed in ionic compounds.[8] These can be explained by lattice thermal expansion,[9] another phonon effect. We present temperature-dependent soft-x-ray emission (SXE) and soft-x-ray absorption (SXA) measurements on MgO, α-Al_2O_3, and α-SiO_2. These measurements show, in detail, the final-state effects on phonon coupling for transitions involving the Mg $2P$ core hole in MgO. In addition, we report the temperature dependence of emission and absorption features for MgO, α-Al_2O_3, and α-SiO_2.

The experiments were performed on beam line U10A at the National Synchrotron Light Source, Brookhaven National Laboratory. Both the SXE and SXA measurements were made on the same soft-x-ray spectrometer.[10] This spectrometer is a 5-m-radius toroidal grating with Rowland optics. The resolution over the range studied was approximately 0.1 eV. Electrons of 1 keV, 10 μA, were used to excite the cation $2P$ core states during the SXE measurements. Reflectivity was measured by reflecting white light from the synchrotron, off the sample, and into the spectrometer. SXA spectra were derived from these reflectivities using the approximation that $R \propto \mathcal{E}_2^2$, where R is the reflectivity, and $\mathcal{E}_2$ is the absorption. It has been shown[11] that this is an accurate method for measuring SXA. High-purity single crystals were purchased from Electronic Space Products International. The samples were firmly clamped to a Ta sheet which was heated by electron bombardment. Sample temperature was measured using a Chromel-Alumel thermocouple, clamped to the front of the sample by a thin Ta bar.

When the electronic state of an atom in a solid is changed the atomic equilibrium positions near the excited atom are altered. The lattice cannot relax during the time period of the electronic transition. This results in the creation of phonons in the final state. In general, there is a distribution in the number of phonons created, which leads to a broadening of the electronic transition spectrum. In ionic solids the core hole interacts primarily with longitudinal optical (LO) phonons and, since these bands have little dispersion, an Einstein lattice is an excellent approximation. In the linear coupling approximation the standard deviation of the phonon broadening (σ_{ph}) as a function of temperature is given by[7]

$$\sigma_{ph}^2 = \hbar\omega_{LO}\Sigma_{ph}\coth(\hbar\omega_{LO}/2kT)\,, \tag{1}$$

where Σ_{ph} is the relaxation energy (sometimes referred to as the phonon self-energy) of the final state. The relaxation energy is the energy difference between the fully relaxed final state (atoms in new equilibrium position) and the final state immediately after a Frank-Condon transition. All else being equal, the larger the change in atomic equilibrium positions, the larger the relaxation energy.

As the temperature of a solid increases inharmonic phonon effects cause the lattice to expand. This change in lattice constant has an additional effect on electronic transitions. For ionic compounds, the energy position and widths of bands are sensitive to lattice spacing.[9] These effects can be understood with the tight-binding model, considering nearest-neighbor interactions only, although the real situation is more complicated. Increasing the lattice constant reduces the magnitude of the overlap integrals. This decreases the bands dispersion and shifts them in energy. The direction of the energy shifts are determined by the sign of the overlap integral. Temperature-dependent optical-reflectivity measurements on MgO and α-Al_2O_3 (Ref. 8) have shown that the band gap decreases with temperature. Also, features in the joint density of states (optical reflectivity) of MgO and α-Al_2O_3 have been observed[8] to shift in energy with temperature.

SXE and SXA spectra for MgO are shown in Fig. 1 for two sample temperatures. The SXE spectra have been divided by E^3, where E is the photon energy, to approximate the density of states. The Mg $2P \rightarrow 2S$ radiative

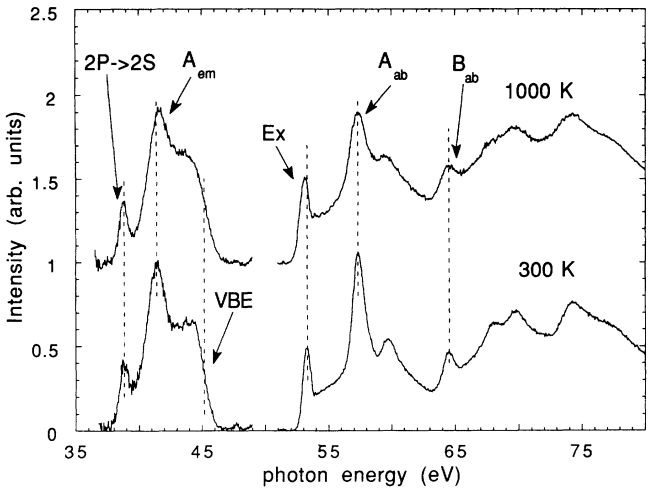

FIG. 1. SXE and SXA spectra of MgO obtained at room temperature (bottom) and at 1000 K (top). The SXE spectra have been divided by E^3 to approximate the density of states.

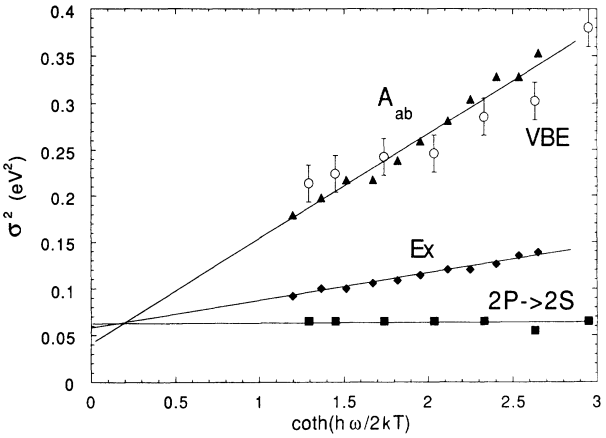

FIG. 2. Temperature-dependent widths of spectral features, A_{ab} (▲), VBE (◊), Ex (◆), and $2P \rightarrow 2S$ (■). Linear fits are shown for A_{ab}, Ex, and $2P \rightarrow 2S$ features.

core-core transition appears near 39 eV in the SXE spectra (Fig. 1). The peak near 53.5 eV in the SXA spectra has been identified as the Mg $L_{2,3}$ exciton.[11] As the temperature is increased, both the SXE and SXA spectra are observed to change. In SXE the valence-band edge (VBE) is broadened and shifted towards higher energies while no energy shift or broadening is observed for the $2P \rightarrow 2S$ core-to-core transition. The peak labeled A_{em} shifts towards higher energies. In SXA, the exciton (Ex) is broadened and shifted to lower energies while the peak labeled A_{ab} is broadened but not shifted. Other features in the SXA spectrum, including B_{ab}, are broadened but not shifted.

The various features defined in Fig. 1 were fitted with a least-squares routine to determine both their temperature-dependent broadening and energy shifts. The $2P \rightarrow 2S$ core-to-core transition and the absorption feature A_{ab} were fitted with a pair of Gaussians of variable but equivalent width, a spin-orbit splitting of 0.28 eV, and the statistical $I(L_3)/I(L_2)$ intensity ratio of 2. A linear background was used for both of these fits. The VBE was fitted with a density of states proportional to $(E_{VBM}-E)^{1/2}$, where E_{VBM} is the valence-band maximum, a spin-orbit splitting of 0.28 eV, and an $I(L_3)/I(L_2)$ intensity ratio of 2, all convoluted with a Gaussian of variable width. The exciton was fitted with a pair of Gaussians of variable but equivalent width, a spin-orbit splitting of 0.28 eV, and a nonstatistical $I(L_3)/I(L_2)$ intensity ratio of 0.2. This nonstatistical ratio is a result of the exchange energy being similar in magnitude to the spin-orbit energy.[11] Varying this ratio between 0.0 and 0.5 has no significant effect on our results. The first moments of the peaks labeled A_{em} and B_{ab} in Fig. 1 were determined with Gaussian fits. No broadening measurements of these peaks were attempted due to the uncertainty in background. Likewise, no fits were attempted for the other features in the SXA spectrum due to overlap and uncertainties in background.

Temperature-dependent broadenings of electronic transitions in MgO are reported in Fig. 2. The relaxation energies for the various transitions are derived from the data in Fig. 2 using (1) and are reported in Table I. An LO phonon energy of 60 meV, X point, was used.[12] It should be noted that the relaxation energy, determined in this manner, is not sensitive to the choice of ω_{LO} since $\coth(\hbar\omega_{LO}/2kT) \approx 2kT/\hbar\omega_{LO}$ for $\hbar\omega_{LO} \ll 2kT$. The common, $T=0$, intercept is due to instrumental resolution and inhomogeneous broadening. The relaxation energies in Table I can be understood by assuming that the MgO lattice consists of point ions and by considering the effects of each electronic transition on the equilibrium position of the nearest neighbors. For the $2P \rightarrow 2S$ transition Σ_{ph} is negligible (Table I). The charge of the Mg ion does not change during this transition and therefore the nearest-neighbor equilibrium distances are not affected. For absorption into the state A_{ba} ($\Sigma_{ph}=2.1$ eV), the charge on the Mg ion changes from +2 to +3 and the nearest-neighbor equilibrium distances are greatly affected. The relaxation energy for the transition into the exciton state is 0.5 eV. Here the nearest neighbors see an effective charge of between +2 and +3 in the final state since the exciton is highly localized and screens the core hole. Nearest-neighbor equilibrium distances are affected, but not as much as by absorption into A_{ab}. The uncertainties in the VBE measurements are large due to the movement of the edge with temperature; however, the resulting value of Σ_{ph} is the same as for absorption into the A_{ab} state within our experimental uncertainty. It is significant that the same temperature-dependent broadening is measured for the VBE as for A_{ag}. This suggests that partial relaxation effects[13] are not important for Mg $2P$ SXE.

TABLE I. Phonon relaxation energies Σ_{ph} for electronic transitions in MgO, α-Al_2O_3, and α-SiO_2. Transitions are identified in Figs. 1 and 3; values are given in eV.

	$2P \rightarrow 2S$	VBE	Ex_{core}	A_{ab}
MgO	<0.04	1.5 ± 0.5	0.5 ± 0.05	2.1 ± 0.2
α-Al_2O_3	· · ·	1.6 ± 0.6	0.4 ± 0.2	· · ·
α-SiO_2	· · ·	<1.0	<0.2	· · ·

We have interpreted the different relaxation energies, obtained for absorption into the exciton and A_{ab} state, as due to exciton screening of the core hole. The exciton wave function should therefore be localized primarily within one lattice spacing of the Mg ion. This is consistent with the size of the exciton determined through comparison of the exciton energy with the first allowed $2p^6 \rightarrow 2p^5 3s^1$ transition in gas phase Mg^{2+}. These transitions are within 0.15 eV of each other at room temperature,[11] suggesting that the spatial extent of the exciton is less than a lattice spacing. If the exciton were larger than a lattice spacing, the O^{2-} $2P$ states would screen the exciton, changing the energy from what is observed in the gas phase. The screening of the core hole potential by the exciton state is not complete, however. This is evident in the slight broadening with temperature of the exciton transition.

Phonon relaxation energies in ionic crystals have been estimated by Citrin, Eisenberger, and Hamann[3] (CEH) using polaron theory,[14] with reasonable success. Here the long-range Coulomb potential of the core hole is assumed to interact with the ionic polarizability of the lattice. The core hole potential interacts primarily with LO phonons. Due to the low dispersion of LO phonons, all phonons are considered to have the same frequency. In the strong-coupling limit,[14] assuming a Debye cutoff for the phonon wave vector, the relaxation energy is[3]

$$\Sigma_{ph} = e^2(6/\pi V_m)^{1/2}(1/\epsilon_\infty - 1/\epsilon_0) , \quad (2)$$

where V_m is the primitive cell volume, ϵ_∞ is the high-frequency dielectric constant (n^2), and ϵ_0 is the static dielectric constant. For MgO we obtain $\Sigma_{ph}=1.6$ eV. This should be compared with our measured value of $\Sigma_{ph}=2.1$ eV for absorption into state A_{ab} (ionized core hole). This is consistent with the trend found by CEH when comparing their results on alkali halides to this model; the model underestimates the relaxation energy. More recently, Mahan has obtained closer fits to the available alkali halide data using a multimode model. In his analysis, Mahan[4] determined that LO phonons at X provide the important temperature dependence to the linewidth. We are not aware of any such calculations on MgO although Mahan's model, which considers localized holes in a point-ion lattice, should be applicable for MgO.

Similar measurements were made on α-Al_2O_3 and α-SiO_2. Shown in Fig. 3 are the room-temperature SXE/E^3 and SXA spectra for α-Al_2O_3 and α-SiO_2. Relaxation energies were determined for the VBE and exciton transitions for α-Al_2O_3. These relaxation energies are reported in Table I. The relaxation energy for the exciton transition, 0.4 eV, is less than the relaxation energy for the VBE transition, 1.6 eV. This is similar to what was found for MgO and suggests that the Al L exciton is localized primarily within a nearest-neighbor distance. No changes were observed in either the SXE or SXA spectra of α-SiO_2 over the temperature range studied, 300–1000 K. The large experimental upper limit in Σ_{ph} for the VBE transition, 1.0 eV, is due to the broad shape of the α-SiO_2 VBE.

The temperature dependence of the electronic transition energies for MgO are presented in Fig. 4. Here the transition energies are shown relative to the $T=300$ K values, so that all the information can be contained on one graph. As the temperature increases, the VBM and the A_{em} feature move to higher energies, while the exciton moves to lower energies. We detect no shift for the $2P \rightarrow 2S$ transition or the A_{ab} and B_{ab} features. These transitions are omitted from Fig. 4 for brevity. The results presented in Fig. 4 were fit with a linear least-squares routine. The temperature coefficients are presented in Table II. Similar measurements were made on α-Al_2O_3 and α-SiO_2. Linear temperature coefficients for the transitions identified in Fig. 3 are presented in Table II. For α-Al_2O_3 the VBM and other emission features move to higher energies with an increase in temperature while the exciton moves to lower energies. We observe no temperature-dependent shift in the α-SiO_2 SXE and SXA spectra. The absence of a temperature-dependent shift can be ex-

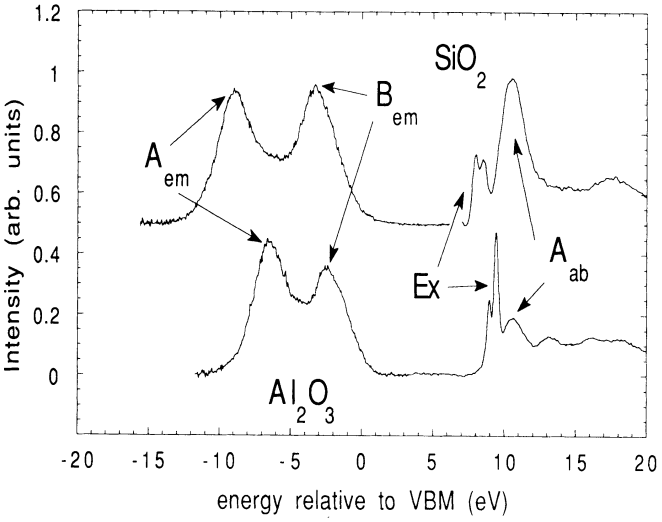

FIG. 3. Room-temperature SXE/E^3 and SXA of α-SiO_2 (top) and α-Al_2O_3 (bottom). The relaxation energies and temperature coefficients for the electronic transitions identified are listed in Tables I and II, respectively.

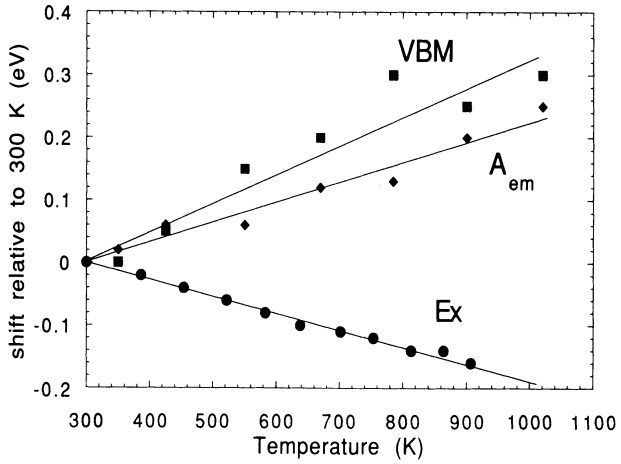

FIG. 4. Temperature dependence of VBM (■), A_{em} (◆), and Ex (●) transition energies of MgO. Transition energies are shown relative to their values at 300 K.

TABLE II. Linear temperature coefficients for electronic transitions of MgO, α-Al_2O_3, and α-SiO_2. Values for Ex_{val} are from Ref. 8. Transitions are identified in Figs. 1 and 3; values are in meV/K.

	$2P \rightarrow 2S$	A_{em}	B_{em}	VBE	Ex_{core}	A_{ab}	B_{ab}	Ex_{val}
MgO	0 ± 0.03	0.32 ± 0.03	· · ·	0.45 ± 0.1	-0.26 ± 0.02	0 ± 0.05	0 ± 0.05	-0.91
α-Al_2O_3	· · ·	0.24 ± 0.03	0.2 ± 0.02	0.39 ± 0.04	-0.49 ± 0.05	-0.5 ± 0.1	· · ·	-1.0
α-SiO_2	· · ·	0 ± 0.05	0 ± 0.05	0 ± 0.05	0 ± 0.05	0 ± 0.05	· · ·	· · ·

plained by the low thermal expansion coefficient of α-SiO_2, 0.6×10^{-6}/°C, as compared to 7×10^{-6}/°C and 13×10^{-6}/°C for α-Al_2O_3 and MgO, respectively. These transition energies are all relative to the cation $2P$ electron binding energy. This binding energy is also temperature dependent. Therefore, it is the relative temperature dependence of these different transitions that are important when comparison is made to band-structure calculations.

For interband transitions in MgO we have temperature coefficients of -0.32 for $A_{em} \rightarrow A_{ab}$ and $A_{em} \rightarrow B_{ab}$ and -0.45 meV/K for VBM $\rightarrow A_{ab}$ and VBM $\rightarrow B_{ab}$. These values are smaller, by about a factor of 2, than values obtained for features in the joint density of states by optical reflectivity.[8] The reason for this discrepancy could be in the optical data's uncertainty. The optical data records the joint density of states, a convolution of the valence-band and conduction-band density of states. The features are broad and overlap, especially at high temperatures.[8] This would make it difficult to accurately determine the energy of a transition. On the other hand, we are measuring the valence-band and conduction-band density of states separately. The features we have discussed do not overlap significantly with other features. We are not aware of any published temperature-dependent interband transition energies for α-Al_2O_3 and α-SiO_2. These optical spectra are composed of broader features than the spectrum of MgO, making it more difficult to determine a temperature coefficient. For α-Al_2O_3 information is available for the temperature dependence of the valence exciton,[8] which is easier to identify since it is at the threshold.

The temperature coefficient for the Mg L exciton, relative to the VBM, is -0.71 ± 0.1 meV/K. This is identical, within experimental uncertainty, to the temperature coefficient of the MgO valence exciton, -0.91 meV/K.[8] (Unfortunately, no uncertainty was given for the valence exciton's temperature coefficient. However, inspection of the $\mathcal{E}_2$ results published in Ref. 8, especially at higher temperatures, suggest an uncertainty at least as large as ours.) For α-Al_2O_3, the temperature coefficient for the Al L exciton, relative to the VBM, is -0.88 ± 0.07 meV/K. This is also identical, within experimental uncertainty, to the temperature coefficient of the α-Al_2O_3 valence exciton, -1.0 meV/K.[8] Now the valence exciton is nearly degenerate with the fundamental band gap, so that the temperature dependence of the band gap and valence exciton should be identical. This implies that the core exciton follows the conduction-band minimum, i.e., it has a temperature independent binding energy. This information leads us to regard the Mg L (Al L) exciton in MgO (α-Al_2O_3) as a state pulled down from the bottom of the conduction band, Γ point, by the core hole potential. Other evidence for this is the similarity of the exciton energy to the $2p^6 \rightarrow 2p^5 3s^1$ transition in gas phase Mg^{2+} (Al^{3+}) (Ref. 11) and calculations which show that the bottom of the conduction band has a high percentage of Mg (Al) $3s$ character.[15]

In summary, we have quantified the phonon effects on a number of electronic transitions of MgO, α-Al_2O_3, and α-SiO_2. We have shown, in detail, that the final state has a strong effect on the phonon broadening in MgO. This broadening can be understood with a simple model which considers the change in effective charge on the Mg site during an electronic transition. Temperature-dependent shifts of electronic transition energies of MgO, α-Al_2O_3, and α-SiO_2 were presented. For MgO (α-Al_2O_3) the Mg L (Al L) exciton follows the conduction-band minimum. This suggests that these excitons are derived from conduction-band states associated with the Γ-point minimum. For α-SiO_2, we observe no temperature-dependent changes in SXE or SXA. The lack of temperature-dependent shifts is due to the thermal expansion coefficient of α-SiO_2 being much less than the thermal-expansion coefficients of MgO and α-Al_2O_3.

This work was supported by NSF Grant No. DMR-8715430, and the National Institute of Standards and Technology.

[1] L. G. Parratt, Rev. Mod. Phys. **31**, 616 (1959).
[2] L. Hedin and A. Rosengren, J. Phys. F **7**, 1339 (1977).
[3] P. H. Citrin, P. Eisenberger, and D. R. Hamann, Phys. Rev. Lett. **33**, 965 (1974).
[4] G. D. Mahan, Phys. Rev. B **21**, 4791 (1980).
[5] R. D. Carson and S. E. Schnatterly, Phys. Rev. B **39**, 1659 (1989).
[6] D. M. Riffe, G. K. Wertheim, and P. H. Citrin, Phys. Rev. Lett. **67**, 116 (1991).
[7] D. B. Fitchen, in *Physics of Color Centers*, edited by W. B. Fowler (Academic, New York, 1968), p. 293.
[8] M. L. Bortz *et al.*, Phys. Scr. **41**, 537 (1990).
[9] N. W. Ascroft and N. D. Mermin, *Solid State Physics* (Saunders, Philadelphia, 1976), pp. 181–187, 382.
[10] T. A. Callcott *et al.*, Rev. Sci. Instrum. **57**, 2680 (1986); Nucl. Instrum. Methods, Phys. Res. Sect. B **40/41**, 398 (1989).
[11] W. L. O'Brien *et al.*, Phys. Rev. B **44**, 1013 (1991).
[12] S. K. Argarwal, Solid State Commun. **39**, 513 (1981).
[13] C.-O. Almbladh, Phys. Rev. B **16**, 4343 (1977).
[14] T.-D. Lee and D. Pines, Phys. Rev. **92**, 883 (1953).
[15] I. P. Barta, J. Phys. C **15**, 5399 (1982).